



Multi-Scale Modeling of Plutonium Radiation Chemistry in Nitric Acid Solutions. 1. Cobalt-60 Gamma Irradiation of Pu(IV)

April 2024

Changing the World's Energy Future

Gregory Peter Holmbeck, Amy Elizabeth Kynman, Travis S Grimes, Jacy Kathleen Conrad, Simon M Pimblott



DISCLAIMER

This information was prepared as an account of work sponsored by an agency of the U.S. Government. Neither the U.S. Government nor any agency thereof, nor any of their employees, makes any warranty, expressed or implied, or assumes any legal liability or responsibility for the accuracy, completeness, or usefulness, of any information, apparatus, product, or process disclosed, or represents that its use would not infringe privately owned rights. References herein to any specific commercial product, process, or service by trade name, trade mark, manufacturer, or otherwise, does not necessarily constitute or imply its endorsement, recommendation, or favoring by the U.S. Government or any agency thereof. The views and opinions of authors expressed herein do not necessarily state or reflect those of the U.S. Government or any agency thereof.

**Multi-Scale Modeling of Plutonium Radiation
Chemistry in Nitric Acid Solutions. 1. Cobalt-60
Gamma Irradiation of Pu(IV)**

**Gregory Peter Holmbeck, Amy Elizabeth Kynman, Travis S Grimes, Jacy Kathleen
Conrad, Simon M Pimblott**

April 2024

**Idaho National Laboratory
Idaho Falls, Idaho 83415**

<http://www.inl.gov>

**Prepared for the
U.S. Department of Energy
Under DOE Idaho Operations Office
Contract DE-AC07-05ID14517, DE-AC07-05ID14517**

Multi-Scale Modeling of Plutonium Radiation Chemistry in Nitric Acid Solutions. 1. Cobalt-60 Gamma Irradiation of Pu(IV)

Amy E. Kynman,^{a,b} Travis S. Grimes,^{a*} Jacy K. Conrad,^a Simon M. Pimblott,^a and Gregory P. Horne^{a*}

^a*Center for Radiation Chemistry Research, Idaho National Laboratory, 1955 N. Freemont Ave., Idaho Falls, ID, 83415, USA.*

^b*Glenn T. Seaborg Institute, Idaho National Laboratory, Idaho Falls, ID, 83415, USA.*

*Corresponding authors. E-mail: travis.grimes@inl.gov and gregory.holmbeck@inl.gov

ORCID

Amy E. Kynman	0000-0003-4532-5792
Travis S. Grimes	0000-0003-2751-0492
Jacy K. Conrad	0000-0002-0745-588X
Simon M. Pimblott	0000-0001-9169-3030
Gregory P. Horne	0000-0003-0596-0660

ABSTRACT

Careful manipulation of plutonium oxidation states is essential in the study and utilization of its rich redox chemistry. To achieve this level of control, a comprehensive mechanistic understanding of radiation-induced plutonium redox chemistry is critical due to the unavoidable exposure of plutonium to ionizing radiation fields, both inherent and from in-process applications. To this end, we have developed an experimentally evaluated multi-scale computer model for the prediction of gamma radiation-induced Pu(IV) redox chemistry in concentrated nitric acid solutions (1.0, 3.0, and 6.0 M). Under these acidic, aqueous solution conditions, cobalt-60 gamma irradiation afforded marginal net conversion of Pu(IV) to Pu(VI), the extent of which was dependent on the concentration of HNO₃ and absorbed gamma dose. Multi-scale calculations, which are in excellent agreement with experimental data, indicate that this observation is due to a combination of inherent plutonium disproportionation reactions and several radiation-induced processes, including: redox cycling between Pu(IV) and Pu(III), as achieved by the reduction of Pu(IV) by nitrous acid and hydrogen peroxide, and the oxidation of Pu(III) by nitrate and hydroxyl radicals; and the sequential oxidation of Pu(IV) to Pu(V) and Pu(VI) by the remaining available yield of nitrate radicals.

INTRODUCTION

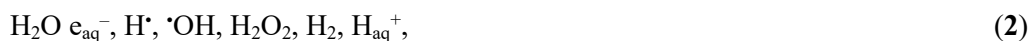
Plutonium (Pu) plays a key role in global actinide research, and over the last 70 years it has been integral in the development of several technologies that have changed the world, including atomic weapons, nuclear fission power reactors, and radioisotope thermoelectric generators for space

exploration.¹⁻³ Despite the importance of these technologies, our fundamental understanding of plutonium chemistry is still far from complete, a testament to this element's unique and complex properties.^{2, 4} One such characteristic is plutonium's ability to coexist as multiple oxidation states in aqueous solution:⁵



a consequence of the redox potentials of its tri- (Pu(III)/Pu³⁺), tetra- (Pu(IV)/Pu⁴⁺), penta- (Pu(V)/PuO₂⁺), and hexa- (Pu(VI)/PuO₂²⁺) oxidation states being very similar ($E^\circ \sim 1$ V).¹ The overall equilibrium shown in **Eq. 1** is achieved through a series of non-elementary reactions involving these plutonium oxidation states and various solvent and solute molecules.^{2, 4}

This distinctive chemical behavior is further complicated in radiation environments, such as those arising from plutonium's inherent nuclear instability. The absorption of ionizing radiation by an aqueous solution leads to water radiolysis (**Eq. 2**) and the formation of several redox active species:⁶



specifically, the reducing hydrated electron (e_{aq}^- , $E^\circ = -2.9$ V) and hydrogen atom (H^\bullet , $E^\circ = -2.3$ V), the strongly oxidizing hydroxyl radical ($\bullet\text{OH}$, $E^\circ = +2.7$ V), and hydrogen peroxide (H_2O_2), which can act as both an oxidant and a reductant depending on solution conditions.⁶ These reactive radiolysis products have the capacity to promote changes in the oxidation state distribution of plutonium ions in aqueous solution, as demonstrated by time-resolved chemical kinetic measurements for several plutonium oxidation states.⁷ These radiation-induced redox reactions can lead to unanticipated chemical reactivity and ultimately complicate attempts to understand, control, and predict plutonium chemistry in the condensed phase.

Despite these implications, few steady-state irradiation studies can be found in the literature, and these are essentially limited to the impact of plutonium oxidation states on the yields of radiolysis products accompanied by mechanistic speculation.⁸⁻²¹ Although these data have been useful for the construction of empirical and stochastic models, they are insufficient for the development of a predictive, mechanistic, multi-scale model. Multi-scale models for radiation effects are important as they capture the fundamental chemistry of an irradiated system from the point of energy deposition, through the lifetime of the non-homogeneous radiation track (microseconds in water), and into homogenous bulk solution (steady-state). The radiation-induced chemistry occurring in each of these time regimes is distinctly different and can be influenced by the presence of solutes.²² Such predictive models can provide significant fundamental insight into the underlying mechanisms of an irradiated system.²³⁻²⁵ For example, multi-scale computer models have been developed and successfully used to interpret and predict radiation-induced changes in the oxidation state distribution of plutonium's adjacent neighbors, neptunium and americium, in aqueous nitric acid (HNO_3) solutions^{26, 27}—the prototypical solvent for

actinide manipulations in nuclear fuel cycle technologies. The reported calculations accurately reproduced experimental behavior and confirmed the fundamental radiation-induced mechanisms responsible for the observed changes in the oxidation state distribution of both actinides. These multi-scale models ultimately provided much needed direction for the development of real-world actinide separations strategies and technologies.

To date, no such radiation chemistry modeling capability exists for plutonium in aqueous solution. In comparison to the aforementioned neptunium and americium studies, wherein up to two chemically active oxidation states were present at a given time, plutonium's multiple, coexisting, and chemically active oxidation states, which comprise of bare ions and dioxo cations (**Eq. 1**), provide additional redox pathways that can complicate radiation-induced competition kinetics.⁷ Consequently, comprehensive fundamental knowledge in this area is essential for the advancement of plutonium science. To this end, we present the first ever multi-scale computer model for the radiation-induced chemistry of Pu(IV) in aqueous HNO₃ solutions (1.0, 3.0, and 6.0 M) experimentally supported by new data from complimentary cobalt-60 gamma irradiation experiments.

MATERIALS AND METHODS

Caution! The plutonium-239 ($\tau_{1/2} = 24,110$ years, $E_{\alpha} = 5.20$ MeV) solutions used in this work were radioactive. Handling was performed in dedicated radiological and nuclear facilities using well-established radiological safety protocols.

Chemicals. Calcium nitrate (Ca(NO₃)₂, $\geq 99.0\%$), hydrochloric acid (HCl, $\geq 99.999\%$ trace metals basis), L-ascorbic acid ($\geq 99.0\%$), nitric acid (HNO₃, $\geq 99.999\%$ trace metals basis), sodium hydroxide (NaOH, 50% in H₂O), sodium nitrite (NaNO₂, $\geq 99.999\%$ trace metals basis), and potassium oxalate (K₂C₂O₄, 99% ACS reagent) were supplied by MilliporeSigma (Burlington, MA, USA). Sodium bismuthate (NaBiO₃, 93% ACS grade) was procured from Chemsavers (Bluefield, VA, USA).

Plutonium Sample Preparation. On hand plutonium-239 stock solutions at the Idaho National Laboratory (INL) Radiochemistry Laboratory were concentrated in HNO₃ media using Eichrom Technologies (Lisle, Illinois, USA) TEVA columns. The initial aqueous plutonium solutions were adjusted to 3.0 M HNO₃ and 0.1 M NaNO₂ prior to loading onto the TEVA column. Once loaded, the column was flushed sequentially with 10 mL of 3.0 M HNO₃ and 10 mL of 6.0 M HCl to remove the background electrolyte and any impurities in the plutonium stock solution. The plutonium was then eluted from the column with 10 mL of 1.0 M HCl. Following this pre-concentration step, the resulting Pu/HCl stock solution was then passed through an AG1-X8 (100-200 mesh) anion exchange resin column to exchange the background chloride anion electrolyte for nitrate ions (NO₃⁻). The AG1-X8 column was first rinsed with 25 mL 2.0 M HNO₃ to convert to the NO₃⁻ form. The column was then conditioned by

rinsing with 25 mL 3.5 M $\text{Ca}(\text{NO}_3)_2$ in 2.0 M HNO_3 .²⁸ The Pu/HCl stock was modified by adjusting the solution sequentially to 3.5 M $\text{Ca}(\text{NO}_3)_2$, 0.2 M L-ascorbic acid (for reduction to Pu(III)), 0.25 M NaNO_2 (for subsequent oxidation to Pu(IV)), and 2.0 M HNO_3 , and then loaded onto the column. The column was then washed with 50 mL 3.5 M $\text{Ca}(\text{NO}_3)_2$ in 2.0 M HNO_3 to remove all impurities, and the ^{239}Pu was then recovered by eluting with 30 mL of 0.35 M HNO_3 (60 °C) into a concentrated aqueous HNO_3 reservoir. The Pu/ HNO_3 eluent was then concentrated by reducing the volume to ~5.5 mL through gentle heating. The final Pu concentration was characterized by quantitatively oxidizing a diluted aliquot of Pu(IV)/ HNO_3 with NaBiO_3 and then measuring the optical absorbance of Pu(VI) at $\lambda_{\text{max}} = 830$ nm ($\epsilon = 118 \text{ M}^{-1} \text{ cm}^{-1}$)²⁹ using an Agilent Technologies (Santa Clara, CA, USA) Cary-6000i UV-vis-nIR spectrophotometer. The concentration of plutonium determined in this way was 10.65 mM. The final concentration of HNO_3 in the concentrated Pu(IV)/ HNO_3 eluent was also determined. This involved adding 0.092 μL of the Pu(IV)/ HNO_3 eluent to 20 mL of 1.0 M $\text{K}_2\text{C}_2\text{O}_4$ at pH 7 and then titrating with 0.1 M NaOH solution to determine a HNO_3 concentration of 6.111 ± 0.068 M. The characterized Pu(IV)/ HNO_3 eluent was then used to prepare all subsequent solutions irradiated in this study by serial dilution.

Table 1. Wavelengths and molar extinction coefficients used in the calculation of plutonium oxidation state concentrations from optical spectra as a function of absorbed gamma dose. Molar extinction coefficients were sourced from references.^{29, 30}

Oxidation state (λ_{max})	Molar extinction coefficient (ϵ , $\text{M}^{-1} \text{ cm}^{-1}$)		
	1.0 M HNO_3	3.0 M HNO_3	6.0 M HNO_3
Pu(IV) (475 nm)	81	80	79
Pu(VI) (830 nm)	117	117	118

Gamma Irradiations. Cobalt-60 ($\tau_{1/2} = 5.27$ years, $E_{\gamma 1} = 1.17$ MeV and $E_{\gamma 2} = 1.33$ MeV) gamma irradiations were performed using the INL Center for Radiation Chemistry Research Nordion (Ottawa, Canada) Gammacell 220E Cobalt-60 irradiator. Samples for irradiation comprised of 1.0 mL of Pu(IV)/ HNO_3 solution sealed in 1.0 cm optical pathlength, screwcap sealed, Spectrosil quartz, semi-micro, Starna Scientific Ltd. (Ilford, United Kingdom) cuvettes. Sample cuvettes were loaded three at a time into a glass beaker positioned at the center of the gamma irradiator chamber, exposed to the instrument's gamma radiation field for approximately 20 hours, and then analyzed for changes in the oxidation state distribution of Pu(IV) using a collocated Agilent Technologies Cary-6000i UV-vis-nIR spectrophotometer. These spectra are given in **Figures S1–S3** in the *Supplementary Information* (SI).

Gamma irradiation dose rates were determined by Fricke solution dosimetry³¹ corrected for the decay of cobalt-60 and HNO_3 solution density vs. water, affording an average dose rate of 35.2 Gy min^{-1} , and a total dose of up to 4.8 kGy. Following baseline corrections, the concentration of Pu(IV) and Pu(VI) were calculated using the wavelength and molar extinction coefficients (ϵ) summarized in **Table 1**. No

other plutonium oxidation states were identified in the absorbance spectra.

Complimentary controls were also run, in which non-gamma-irradiated Pu(IV)/HNO₃ samples were analyzed repeatedly over a 24-hour period to determine the extent of any thermal-chemistry-driven changes on the oxidation state distribution of plutonium. These controls also accounted for the very minor (2–6 Gy) alpha radiolysis contribution from the natural decay of ²³⁹Pu and its daughter nuclides. The absorption spectra for these experiments are given in **Figures S4–S6** in the SI.

Multi-Scale Computer Model Calculations. Monte Carlo radiation track structure^{32, 33} and independent reaction times (IRT)³⁴ models were used in conjunction with a deterministic reaction kinetics model²² to determine the gamma radiation-induced redox chemistry of plutonium in aqueous HNO₃ solutions (1.0, 3.0, and 6.0 M). Radiation track structure simulations were performed for aerated ([O₂] = 0.25 mM), aqueous HNO₃ solution conditions to calculate representative radiolytic yields for each solution permutation, as summarized in **Table S1**. To account for the minor alpha radiolysis contribution from the decay of ²³⁹Pu, alpha radiation track yields were also derived from an array of alpha particle energies (0.1 to 6.0 MeV) and subsequently integrated to 5.20 MeV, given in **Table S2**. The calculated stochastic radiation track yields for water radiolysis were used, in conjunction with direct effect yields for HNO₃ radiolysis from the literature,³⁵ as input parameters in a deterministic reaction kinetics model. The contribution of each set of radiolysis yields was varied by the respective electron fractions of water, NO₃⁻, and HNO₃ for the investigated 1.0, 3.0, and 6.0 M HNO₃ systems. The deterministic model was solved using the FACSIMILE modelling software package (MCPA Software Ltd., Swan Lane Faringdon, UK).³⁶ A complete description of this multi-scale modeling methodology has been previously discussed.²² The chemical reaction kinetics employed by this modelling formulism used existing reaction schemes for water and HNO₃ radiolysis,^{6, 22, 37, 38} in addition to supplementary plutonium + radiolysis product reactions and plutonium equilibria given in **Tables 2** and **3**, respectively.⁷

Table 2. Supplementary plutonium + radiolysis product reaction rate coefficients used in the presented multi-scale model.

Chemical reaction*	Rate coefficient (k , $M^{-1} s^{-1}$)	Reference
$Pu^{3+} + H^{\bullet} \rightarrow Pu^{4+} + H^{-}$	$1.0 \cdot 10^6$	39
$Pu^{3+} + \bullet OH \rightarrow Pu^{4+} + OH^{-}$	$4.2 \cdot 10^8$	40
$Pu^{3+} + NO_3^{\bullet} \rightarrow Pu^{4+} + NO_3^{-}$	$2.5 \cdot 10^8$	41
$Pu^{3+} + H_2O_2 \rightarrow Pu^{4+} + \bullet OH + OH^{-}$	$5.5 \cdot 10^{-2}$	16
$Pu^{3+} + N_2O_4 \rightarrow Pu^{4+} + NO_2^{\bullet} + NO_2^{-}$	$1.0 \cdot 10^{-3}$	42
$Pu^{4+} + H^{\bullet} \rightarrow Pu^{3+} + H_{aq}^{+}$	$2.0 \cdot 10^7$	39
$Pu^{4+} + NO_3^{\bullet} + 2H_2O \rightarrow PuO_2^{+} + NO_3^{-} + 4H_{aq}^{+}$	$1.0 \cdot 10^4$	43
$Pu^{4+} + H_2O_2 \rightarrow Pu^{3+} + HO_2^{\bullet} + H_{aq}^{+}$	0.1	13
$Pu^{4+} + HNO_2 \rightarrow Pu^{3+} + NO_2^{\bullet} + H_{aq}^{+}$	$3.3 \cdot 10^{-2}$	20
$PuO_2^{+} + NO_3^{\bullet} \rightarrow PuO_2^{2+} + NO_3^{-}$	$1.0 \cdot 10^7$	43
$PuO_2^{2+} + H^{\bullet} \rightarrow PuO_2^{+} + H_{aq}^{+}$	$2.0 \cdot 10^8$	39
$PuO_2^{2+} + H_2O_2 \rightarrow PuO_2^{+} + HO_2^{\bullet} + H_{aq}^{+}$	$6.2 \cdot 10^{-3}$	9
$PuO_2^{2+} + HNO_2 \rightarrow PuO_2^{+} + NO_2^{\bullet} + H_{aq}^{+}$	$3.0 \cdot 10^{-2}$	20

* Under the acidic conditions employed here, the plutonium + e_{aq}^{-} reactions were not included. The e_{aq}^{-} is completely scavenged by NO_3^{-} and H_{aq}^{+} ions^{44, 45} as evident from the calculated G -values given in **Tables S1** and **S2**.

Table 3. Plutonium equilibrium constants at 1 M ionic strength used in the presented multi-scale model.

Chemical equilibria	Equilibrium constant ($I = 1 M$) ⁴⁶
$2Pu^{4+} + 2H_2O \rightleftharpoons Pu^{3+} + PuO_2^{+} + 4H_{aq}^{+}$	$6.97 \cdot 10^{-4}$
$Pu^{4+} + PuO_2^{+} \rightleftharpoons Pu^{3+} + PuO_2^{2+}$	13.228

RESULTS AND DISCUSSION

Under the acidic, aqueous HNO_3 solution conditions investigated here, cobalt-60 gamma irradiation afforded only small changes in the initial steady-state redox distribution of plutonium, which initially consisted primarily of Pu(IV) with between approximately 14–17% Pu(VI), as shown in **Fig. 1–3** for 1.0, 3.0, and 6.0 M HNO_3 , respectively. These data were surprising given our previous findings for neptunium and americium ions,^{26, 27, 47, 48} and the existence of experimentally determined chemical kinetics for the reaction of several plutonium oxidation states with aqueous HNO_3 radiolysis products (**Table 2**). The gamma irradiation of plutonium in these concentrated HNO_3 solutions was expected to promote the quantitative conversion of Pu(IV) into a steady-state mixture of Pu(III) and Pu(VI) via H_2O_2/HNO_2 reduction and $\bullet OH/NO_3^{\bullet}$ radical oxidation processes, respectively. Further interrogation of these data by

our multi-scale modeling methods provided greater insight into the apparent resilience of these plutonium systems to steady-state radiation-induced changes in redox distribution.

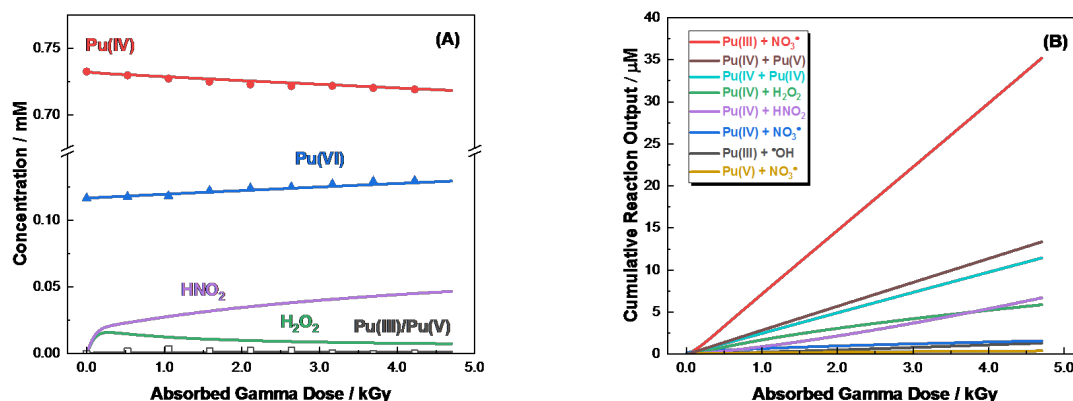


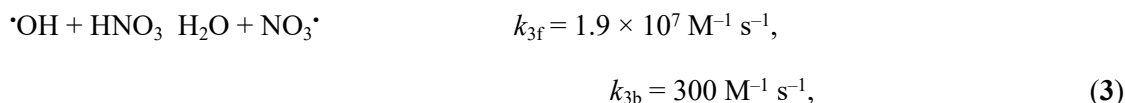
Fig. 1. (A) Concentration of Pu(IV), Pu(VI), and significant ($\geq 1 \mu\text{M}$) radiolysis products as a function of absorbed dose from the gamma irradiation of plutonium in aerated, aqueous 1.0 M HNO₃ solution. Open symbols were determined by plutonium mass balance. Solid curves are predicted values from multi-scale modeling calculations. (B) Cumulative reaction output model predictions as a function of absorbed gamma dose for the irradiation of plutonium in aerated, aqueous 1.0 M HNO₃, showing radiation-induced reactions with cumulative outputs $\geq 1 \mu\text{M}$.

For the gamma irradiation of plutonium in 1.0 M HNO₃ solution, calculations predicted the accumulation of HNO₂[†], the growth and consumption of H₂O₂[†], and a small net conversion of Pu(IV) into Pu(VI) (~11.2% conversion by 4.2 kGy), as shown in **Fig. 1A**. Analysis of the underlying radiation-driven plutonium reactions—expressed as cumulative reaction outputs vs. absorbed gamma dose in **Fig. 1B**—show that Pu(IV) is transiently reduced to Pu(III) by its reactions with H₂O₂ and HNO₂. Additionally, Pu(IV) is also predicted to be transiently oxidized, albeit to a lesser extent, to Pu(V). The oxidation of Pu(IV) is in competition with the scavenging of NO₃[•] radicals by Pu(III), which scavenges ~95% of the available NO₃[•] radical yield under the investigated conditions. The remaining ~5% partially accounts for the net accumulation of Pu(VI) via the oxidation of Pu(V). These radiation-induced processes are augmented by the equilibria given in **Table 2**, ultimately allowing for the Pu(III)-mediated redox cycling mechanism to quantitatively reform Pu(IV), and the net accumulation of Pu(VI). These findings are consistent with our steady-state observations (**Fig. 1A**).

When the concentration of HNO₃ was increased to 3.0 and then 6.0 M, the overall trend in plutonium ion redox distribution with absorbed gamma dose was generally the same as for irradiation in 1.0 M HNO₃, i.e., redox cycling between Pu(IV) and Pu(III), with a small fraction oxidized to Pu(VI). However, there are subtle differences in the underlying mechanisms, in particular the predicted ingrowth of Pu(III) and Pu(V).

[†] Experimental determination of HNO₂ and H₂O₂ was not possible in this study as their absorption profiles were masked by the spectra of the plutonium oxidation states present.

For gamma irradiation in 3.0 M HNO₃ (**Fig. 2**), the radiation-induced chemistry of plutonium is dominated by: the oxidation of Pu(III), Pu(IV), and Pu(V) by NO₃[•] radicals; the reduction of Pu(IV) and Pu(VI) by HNO₂; and the reduction of Pu(IV) by H₂O₂, as shown in **Fig. 2B**. Again, the equilibria in **Table 3** provide a critical role in the redistribution of plutonium oxidation states during the irradiation. Loss of the [•]OH radical-driven Pu(III) oxidation pathway is a consequence of the scavenging of [•]OH radicals by undissociated HNO₃ (HNO₃ ⇌ NO₃⁻ + H_{aq}⁺, pKa ~ 1.37):⁴⁹⁻⁵¹



which affords a concomitant increase in the available yield of NO₃[•] radicals for reaction with plutonium ions (**Table 2**)¹⁵.

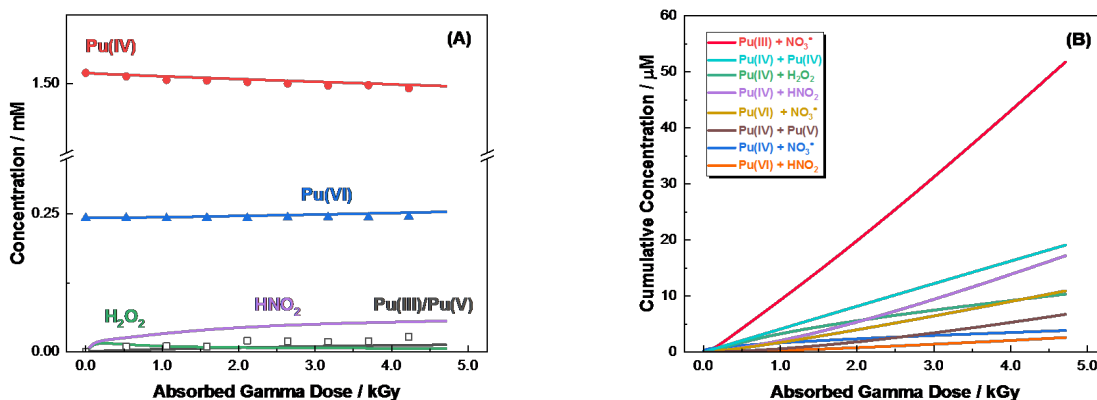
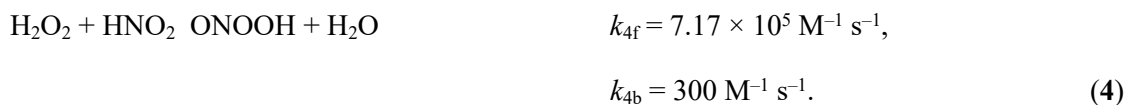


Fig. 2. (A) Concentration of Pu(IV), Pu(VI), and significant ($\geq 1 \mu\text{M}$) radiolysis products as a function of absorbed dose from the gamma irradiation of Pu(IV) in aerated, aqueous 3.0 M HNO₃ solution. Open symbols were determined by mass balance. Solid curves are predicted values from multi-scale modeling calculations. (B) Cumulative reaction output model predictions as a function of absorbed gamma dose for the irradiation of Pu(IV) in aerated, aqueous 3.0 M HNO₃ solution, showing radiation-induced reactions with cumulative outputs $\geq 1 \mu\text{M}$.

The contribution of HNO₂ to the overall reduction of Pu(IV) becomes greater than that afforded by H₂O₂. The re-ordering of reduction reaction importance is due to a decrease in the radiolytic yield of H₂O₂ with increasing HNO₃ concentration (**Table S1** and **S2**). This effect is the consequence of a combination of radiation track scavenging reactions, such as **Eq. 3**, and the decreasing electron fraction of H₂O (0.82 in 3.0 M HNO₃ vs. 0.94 in 1.0 M HNO₃), which ultimately reduces the available yield of H₂O₂ for reaction with plutonium ions (**Table 1**) and HNO₂:^{52, 53}



Furthermore, less Pu(VI) is accumulated (~1.1% conversion by 4.2 kGy) because of the change in acidity in going from 1.0 to 3.0 M HNO₃, which shifts the position of the equilibria in **Table 3**. This effect is

evident from the relative contribution of each equilibrium reaction to the total formation of Pu(VI)/Pu(III) shown in **Fig. 2B**. Interestingly, model predictions indicate the formation of a low, steady-state concentration of Pu(III) and Pu(V) (1.2 and 11.1 μM by 4.2 kGy, respectively), the summation of which is shown in **Fig. 2A**. The accumulation of these two oxidation states could not be quantified from the corresponding absorption spectra (**Fig. S2**). However, the plutonium mass balance for this system provided experimental support for these predictions, as up to 27 mM could not be accounted for by Pu(IV) and Pu(VI). The predicted accumulation of Pu(III) and Pu(V) is another consequence of the shift in the equilibria in **Table 3** with increasing HNO_3 concentration.

In 6.0 M HNO_3 (**Fig. 3**), the contribution of H_2O_2 to plutonium ion redox chemistry is further diminished. We find that under these concentrated HNO_3 conditions the radiation-induced redox chemistry of plutonium is dominated by three processes: the reduction of Pu(IV) and Pu(VI) by HNO_2 , and the oxidation of Pu(III) by NO_3^\cdot radicals to regenerate Pu(IV), as shown in **Fig. 3B**. These underlying mechanisms, in combination with the equilibria in **Table 3**, again, afford the gradual accumulation of Pu(VI) ($\sim 1.4\%$ conversion by 4.6 kGy).

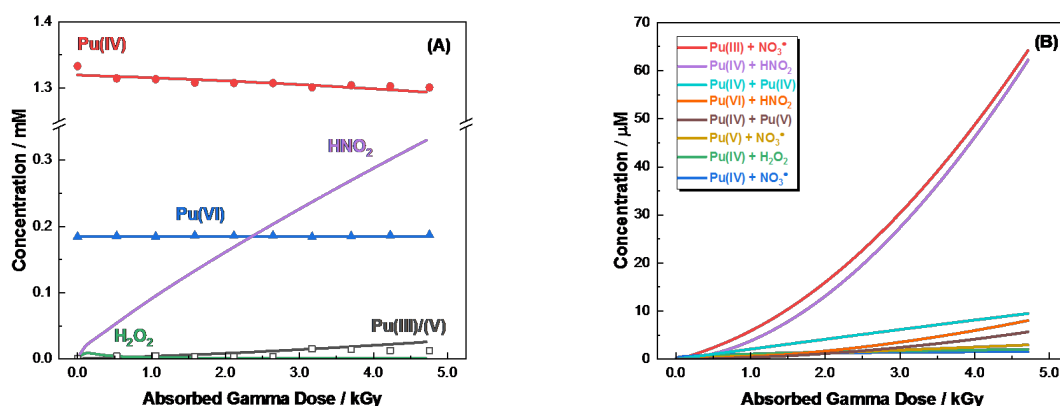


Figure 3. (A) Concentration of Pu(III)/Pu(V), Pu(IV), Pu(VI), and significant ($\geq 1 \mu\text{M}$) radiolysis products as a function of absorbed dose from the gamma irradiation of Pu(IV) in aerated, aqueous 6.0 M HNO_3 solution. Open symbols were determined by mass balance. Solid curves are predicted values from multi-scale modeling calculations. (B) Cumulative reaction output model predictions as a function of absorbed gamma dose for the irradiation of Pu(IV) in aerated, aqueous 6.0 M HNO_3 solution, showing radiation-induced reactions with cumulative outputs $\geq 1 \mu\text{M}$.

As with in the 3.0 M HNO_3 system, calculations again predict the accumulation of Pu(III) and Pu(V) (15.1 and 10.5 μM by 4.7 kGy, respectively). The relatively higher yield of predicted Pu(III) is primarily due to the significant decrease in the radiolytic yield of H_2O_2 (**Table S1**), which in turn inhibits **Eq. 4**. These conditions afford a greater available yield of HNO_2 that promotes more extensive Pu(IV)/Pu(VI) reduction as compared to the 1.0 and 3.0 M HNO_3 systems.

In light of the predicted accumulation of Pu(III) and Pu(V) in these concentrated HNO_3 systems, larger gamma doses will be investigated in the future to determine whether a greater steady-state yield can

be attained and quantified to further validate our model's predictions.

CONCLUSIONS

A multi-scale model has been developed and used to elucidate the fundamental gamma radiation-induced behavior of plutonium ions in concentrated aqueous HNO₃ solutions (1.0, 3.0, and 6.0 M). Excellent agreement was achieved between calculation and experiment for all solution permutations by using previously determined reaction kinetics rate coefficients. Gamma irradiation of the predominantly Pu(IV) solutions afforded negligible (<12%) steady-state changes in the redox distribution of the present plutonium oxidation states. These observations were computationally demonstrated to be a consequence of redox cycling between Pu(IV) and Pu(III), as mediated [•]OH/NO₃[•] radical oxidation of Pu(III), and H₂O₂/HNO₂ driven reduction of Pu(IV). Additionally, the gradual net accumulation of Pu(VI) was facilitated by the oxidation of Pu(V) by the NO₃[•] radical and Pu(IV) mediated. These radiation-induced process were found to be augmented by plutonium equilibria, which were predicted to facilitate the additional accumulation of Pu(III) and Pu(V) with increasing HNO₃ concentration.

The presented data and multi-scale model calculations predominantly account for the effects of low linear energy transfer (LET) radiation (beta and gamma) on the oxidation state distribution of plutonium. As such, these findings are applicable to the self-irradiation of specific plutonium isotopes (e.g., ²⁴¹Pu $\tau_{1/2}$ = 14.35 years, E_{β} = 20.82 keV) and the presence of plutonium ions in radiation environments containing beta/gamma emitting radioisotopes, such as in nuclear waste reprocessing solvent systems and storage tanks. However, the extent of radiation effects on oxidation state distribution of plutonium ions are expected to be strongly dependent on radiation quality (type and energy), which dictates LET and thus, the separation of energy transfer events in a radiation track.⁵⁴ As LET is increased the yields of radical radiolysis products (e.g., NO₃[•] and [•]OH radicals) decrease with a concomitant increase in molecular radiolysis product yields (e.g., HNO₂ and H₂O₂), as demonstrated by the *G*-values in **Tables S1** and **S2**. Therefore, a much higher steady-state concentration of Pu(III) is expected under alpha irradiation conditions, such as from the natural decay of ²³⁹Pu ($\tau_{1/2}$ = 24110 years, E_{α} = 5.24 MeV), which would have significant implications on plutonium redox distribution and chemistry. Consequently, follow on alpha irradiation studies are underway.

AUTHOR INFORMATION

Corresponding Authors

Travis S. Grimes – Center for Radiation Chemistry Research, Idaho National Laboratory, 1955 N. Freemont Ave., Idaho Falls, 83415, USA; orcid.org/0000-0003-2751-0492;
E-mail: travis.grimes@inl.gov

Gregory P. Horne – Center for Radiation Chemistry Research, Idaho National Laboratory, 1955 N. Freemont Ave., Idaho Falls, 83415, USA; orcid.org/0000-0003-0596-0660; E-mail: gregory.holmbeck@inl.gov.

ACKNOWLEDGMENT

This study was supported by the U.S. Department of Energy (DOE) Assistant Secretary for Nuclear Energy, under the Material Recovery and Waste Form Development campaign, and the INL Laboratory Directed Research & Development (LDRD) Program under DOE-Idaho Operations Office Contract DE-AC07-05ID14517. Multi-scale model calculations made use of the resources of the High Performance Computing Center at Idaho National Laboratory, which is supported by the U.S. DOE Office of Nuclear Energy and the Nuclear Science User Facilities under Contract No. DE-AC07-05ID14517.

ASSOCIATED CONTENT

Supporting Information available. UV-Visible absorption spectra used for plutonium quantification; Radiolytic yields calculated by radiation track structure modeling for the gamma and alpha irradiation of aerated, aqueous nitric acid solution.

REFERENCES

- (1) Morss, L. R.; Edelstein, N. M.; Fuger, J. *The Chemistry of the Actinide and Transactinide Elements*; 2006.
- (2) *Plutonium Handbook*. 2nd ed.; American Nuclear Society: USA, 2019; Vol. 1-7.
- (3) Swallow, A. J.; Inokuti, M. Radiation-energy partition among mixture components: Current ideas on an old question. *Radiat. Phys. Chem.* 1988, 32 (2), 185-189.
- (4) D.L. Clark, S. S. H., G.D. Jarvinen, and M.P. Neu. Plutonium. In *The Chemistry of the Actinides and Transactinide Elements, Fourth Edition*, L.R. Morss, N. M. E., and J. Guger Ed.; Springer, 2010.
- (5) Darab, J. G.; Li, H.; Bucher, J. J.; Icenhower, J. P.; Allen, P. G.; Shuh, D. K.; Vienna, J. D. Redox chemistry of plutonium and plutonium surrogates in vitrified nuclear wastes. *JACerS* 2022, 105 (11), 6627-6639.
- (6) Buxton, G. V.; Greenstock, C. L.; Helman, W. P.; Ross, A. B. Critical Review of rate constants for reactions of hydrated electrons, hydrogen atoms and hydroxyl radicals ($\cdot\text{OH}/\cdot\text{O}^-$ in Aqueous Solution. *J. Phys. Chem. Ref. Data.* 1988, 17 (2), 513-886.
- (7) Mincher, B. J.; Mezyk, S. P. Radiation chemical effects on radiochemistry: A review of examples important to nuclear power. *Radiochim. Acta* 2009, 97 (9).
- (8) Kazanjian, A. R.; Horrell, D. R. Radiolytically generated gases in plutonium-nitric acid solutions. *Radiat. Eff.* 1972, 13 (3-4), 277-280.
- (9) Koltunov V.S.; Kulikov, I. A. K., N.V.; Nikishova, L.K. . Kinetics of Pu(IV) reduction by hydrogen peroxide in nitric-acid solution. *Radiokhimiya* 1981, 23, 462-465.
- (10) Kuno, Y.; Hina, T.; Masui, J. Radiolytically Generated Hydrogen and Oxygen from Plutonium Nitrate Solutions. *J. Nucl. Sci. Technol.* 1993, 30 (9), 919-925.
- (11) Liu, Z.; Fang, Z.; Wang, L.; He, H.; Lin, M.-Z. Alpha radiolysis of nitric acid aqueous solution irradiated by ^{238}Pu source. *Nucl. Sci. Tech.* 2017, 28 (4).

- (12) Maillard, C.; Adnet, J. M. Plutonium(IV) peroxide formation in nitric medium and kinetics Pu(VI) reduction by hydrogen peroxide. *Radiochim. Acta* 2001, 89 (8), 485-490.
- (13) Mazumdar, A. S. G.; Vaidyanathan, S. On the Oxidation of Plutonium (III) by Hydrogen Peroxide—Probable Formation of an Unstable Plutonium (III) Peroxy Complex. *Radiochim. Acta* 1973, 19 (4), 165-168.
- (14) N.N. Andreychuk, A. A. F., K.V. Rotmanov, and V.Y Vasiliev. Plutonium(III) Oxidation Under α -Irradiation in Nitric Acid Solutions. *J. Radioanal. Nucl. Chem.* 1990, 143, 427.
- (15) Perrin, B.; Venault, L.; Broussard, E.; Vandendorre, J.; Blain, G.; Fattahi, M.; Nikitenko, S. Influence of plutonium oxidation state on the formation of molecular hydrogen, nitrous acid and nitrous oxide from alpha radiolysis of nitric acid solution. *Radiochim. Acta* 2022, 110 (5), 301-310.
- (16) Pikaev, A. K. S., V.P.; Gogolev, A.V. Radiation chemistry of aqueous solutions of actinides. *Russ. Chem. Rev.* 1997, 1997 (66), 763-788.
- (17) Sheppard, J. C. *Alpha Radiolysis of Plutonium (IV): Nitric Acid Solutions*; BNWL-751; United States, 1968.
- (18) V.S. Koltunov, G. I. Z., V.I. Marchenko, and M.F. Tikhonov. Kinetics and Mechanisms of Some Redox Reactions of Neptunium, Plutonium, and Uranium. *Radiokhimiya* 1975, 17, 301.
- (19) Vladimirova, M. V. Radiation Chemistry of Actinides. *J. Radioanal. Nucl. Chem.* 1990, 143, 445.
- (20) Vladimirova, M. V. Recent achievements of actinide radiation chemistry. *J. Alloys Compd.* 1998, 271, 723-727.
- (21) W.G. Burns, C. E. L., and W.R. Marsh. The self radiolysis of nitric acid solutions of Pu(IV) nitrate. *Eur. Appl. Res. Rept.-Nucl. Sci. Technol.* 1981, 3, 653.
- (22) Horne, G. P.; Donoclift, T. A.; Sims, H. E.; Orr, R. M.; Pimblott, S. M. Multi-Scale Modeling of the Gamma Radiolysis of Nitrate Solutions. *J. Phys. Chem. B.* 2016, 120 (45), 11781-11789.
- (23) Conrad, J. K.; Pilgrim, C. D.; Pimblott, S. M.; Mezyk, S. P.; Horne, G. P. Multiscale modelling of the radical-induced chemistry of acetohydroxamic acid in aqueous solution. *RSC Adv.* 2022, 12 (46), 29757-29766.
- (24) Conrad, J. K.; Mezyk, S. P.; Isherwood, L. H.; Baidak, A.; Pilgrim, C. D.; Whittaker, D.; Orr, R. M.; Pimblott, S. M.; Horne, G. P. Gamma Radiation-Induced Degradation of Acetohydroxamic Acid (AHA) in Aqueous Nitrate and Nitric Acid Solutions Evaluated by Multiscale Modelling. *Chemphyschem* 2023, 24 (5).
- (25) Horne, G. P.; Zalupski, P. R.; Daubaras, D. L.; Rae, C.; Mezyk, S. P.; Mincher, B. J. Radiolytic degradation of formic acid and formate in aqueous solution: modeling the final stages of organic mineralization under advanced oxidation process conditions. *Water Res.* 2020, 186, 116314.
- (26) Horne, G. P.; Grimes, T. S.; Mincher, B. J.; Mezyk, S. P. Reevaluation of Neptunium-Nitric Acid Radiation Chemistry by Multiscale Modeling. *J. Phys. Chem. B.* 2016, 120 (49), 12643-12649.
- (27) Horne, G. P.; Grimes, T. S.; Bauer, W. F.; Dares, C. J.; Pimblott, S. M.; Mezyk, S. P.; Mincher, B. J. Effect of Ionizing Radiation on the Redox Chemistry of Penta- and Hexavalent Americium. *Inorg. Chem.* 2019, 58 (13), 8551-8559.
- (28) Ryan, J. L.; Wheelwright, E. J. Recovery and Purification of Plutonium by Anion Exchange. *Ind. Eng. Chem.* 1959, 51 (1), 60-65.
- (29) Hall, G. R.; Herniman, P. D.; Walter, A. J. *Spectrophotometric Studies of Plutonium in*

- Nitric Acid Solution. Part I*; AERE-C/R-712; Great Britain Atomic Energy Research Establishment, Harwell, Berks, England (United Kingdom), United Kingdom, 1951.
- (30) Myers, M. N. *Absorption Spectra of Plutonium and Impurity Ions in Nitric Acid Solution*; HW-44744; United States, 1956.
- (31) Fricke, H.; Hart, E. J. The Oxidation of Fe⁺⁺ to Fe⁺⁺⁺ by the Irradiation with X-Rays of Solutions of Ferrous Sulfate in Sulfuric Acid. *J. Chem. Phys.* 1935, 3 (1), 60-61.
- (32) Pimblott, S. M.; LaVerne, J. A. Effects of Track Structure on the Ion Radiolysis of the Fricke Dosimeter. *J. Phys. Chem. A* 2002, 106 (41), 9420-9427.
- (33) Pimblott, S. M.; LaVerne, J. A.; Mozumder, A. Monte Carlo Simulation of Range and Energy Deposition by Electrons in Gaseous and Liquid Water. *J. Phys. Chem.* 1996, 100 (20), 8595-8606.
- (34) Clifford, P.; Green, N. J. B.; Oldfield, M. J.; Pilling, M. J.; Pimblott, S. M. Stochastic models of multi-species kinetics in radiation-induced spurs. *J. Chem. Soc., Faraday Trans.* 1986, 82 (9).
- (35) Jiang, P.-Y.; Nagaishi, R.; Yotsuyanagi, T.; Katsumura, Y.; Ishigure, K. γ -Radiolysis study of concentrated nitric acid solutions. *J. Chem. Soc., Faraday Trans.* 1994, 90 (1), 93-95.
- (36) *MCPA Software FACSIMILE Kinetic Modeling Software Package*; (accessed 2023).
- (37) Wolff, R. K.; Aldrich, J. E.; Penner, T. L.; Hunt, J. W. Picosecond pulse radiolysis. V. Yield of electrons in irradiated aqueous solution with high concentrations of scavenger. *J. Phys. Chem.* 2002, 79 (3), 210-219.
- (38) Jonah, C. D.; Miller, J. R.; Matheson, M. S. The reaction of the precursor of the hydrated electron with electron scavengers. *J. Phys. Chem.* 2002, 81 (17), 1618-1622.
- (39) Gogolev, A. V.; Shilov, V. P.; Fedoseev, A. M.; Pikaev, A. K. The study of reactivity of actinide ions towards hydrated electrons and hydrogen atoms in acid aqueous solutions by a pulse radiolysis method. *Int. J. Radiat. Appl. Instrum. C* 1991, 37 (3), 531-535.
- (40) Shilov, V. P.; Fedoseev, A. M.; Pikaev, A. K. Neptunium, plutonium, and uranium ion reactivity to primary water radiolysis products. *Sov. Radiochem. (Engl. Transl.); (United States)* 1985, 27:1, Medium: X; Size: Pages: 117-120 2009-2012-2016.
- (41) Gogolev A.V.; Fedoseev, A. M. P. Reactivity of inorganic free radicals with respect to plutonium (III) in aqueous solutions. *High Energy Chem.* 1988, 21, 401-402.
- (42) Dukes, E. K. Kinetics and Mechanisms for the Oxidation of Trivalent Plutonium by Nitrous Acid. *J. Am. Chem. Soc.* 1960, 82 (1), 9-13.
- (43) Vladimirova, M. V. K., I.A.; Sosnovskij, O.A.; Nikishova, L.K. Radiolytic Pu(VI) reduction and Pu(IV) oxidation in the presence of neptunium in HNO₃ solutions. *Radiochem.* 1982, 24, 322-330.
- (44) Horne, G. P.; Pimblott, S. M.; LaVerne, J. A. Inhibition of Radiolytic Molecular Hydrogen Formation by Quenching of Excited State Water. *J. Phys. Chem. B.* 2017, 121 (21), 5385-5390.
- (45) Gregson, C. R.; Horne, G. P.; Orr, R. M.; Pimblott, S. M.; Sims, H. E.; Taylor, R. J.; Webb, K. J. Molecular Hydrogen Yields from the alpha-Self-Radiolysis of Nitric Acid Solutions Containing Plutonium or Americium. *J. Phys. Chem. B.* 2018, 122 (9), 2627-2634.
- (46) Silver, G. L. *Optimization and plutonium equilibrium*; MLM-2373; TRN: 77-001321; United States, 1976.
- (47) Horne, G. P.; Gregson, C. R.; Sims, H. E.; Orr, R. M.; Taylor, R. J.; Pimblott, S. M. Plutonium and Americium Alpha Radiolysis of Nitric Acid Solutions. *J. Phys. Chem. B* 2017, 121 (4), 883-889.
- (48) Grimes, T. S.; Horne, G. P.; Dares, C. J.; Pimblott, S. M.; Mezyk, S. P.; Mincher, B. J.

- Kinetics of the Autoreduction of Hexavalent Americium in Aqueous Nitric Acid. *Inorg. Chem.* 2017, 56 (14), 8295-8301.
- (49) Davis, W.; De Bruin, H. J. New activity coefficients of 0–100 per cent aqueous nitric acid. *J. inorg. nucl. chem.* 1964, 26 (6), 1069-1083.
- (50) Poskrebyshev, G. A.; Neta, P.; Huie, R. E. Equilibrium constant of the reaction $\cdot\text{OH} + \text{HNO}_3 \rightleftharpoons \text{H}_2\text{O} + \text{NO}_3$. in aqueous solution. *Geophys. Res. Atmos.* 2001, 106 (D5), 4995-5004.
- (51) Garaix, G.; Horne, G. P.; Venault, L.; Moisy, P.; Pimblott, S. M.; Marignier, J. L.; Mostafavi, M. Decay Mechanism of NO_3^* Radical in Highly Concentrated Nitrate and Nitric Acidic Solutions in the Absence and Presence of Hydrazine. *J. Phys. Chem. B* 2016, 120 (22), 5008-5014.
- (52) Katsumura, Y. *The Chemistry of Free Radicals: N-Centered Radicals*; John Wiley & Sons, Inc., 1998.
- (53) Loegager, T.; Sehested, K. Formation and decay of peroxyxynitrous acid: a pulse radiolysis study. *J. Phys. Chem.* 2002, 97 (25), 6664-6669.
- (54) Spinks, J. W. T.; Woods, R. J. *An Introduction to Radiation Chemistry*; Wiley, 1990.